A CFD STUDY OF NATURAL CONVECTION INSIDE A BIPV/T SYSTEM

D. Roeleveld*, R. Kumar, D. Naylor, A.S. Fung
Ryerson University
Toronto Ontario
*droeleve@ryerson.ca

ABSTRACT

Natural convection inside a building integrated photovoltaic/thermal (BIPV/T) system is investigated using computational fluid dynamics (CFD). Normally, BIPV/T systems utilize forced convection in the air channel behind the photovoltaic panel, but this requires fans to move the air through the system. These fans use energy that is being produced by the BIPV/T system. In this study, natural convection is used to investigate if it is feasible to remove the fans and therefore reduce the energy requirement. The thermal behavior inside the BIPV/T system is of interest in this study. COMSOL Multiphysics is used to develop a numerical model to study the heat transfer inside a BIPV/T system using natural convection. This numerical model is validated with some experimental data. A comparison is presented of the temperature profiles and heat fluxes between the natural and forced convection cases.

INTRODUCTION

A building integrated photovoltaic/thermal (BIPV/T) system utilizing natural convection inside the air channel was studied using computational fluid dynamics (CFD). A BIPV/T system is composed of solar photovoltaic panels mounted in front of a building wall/roof with an air channel between the PV panel and the structures of wall or roof. Usually, air is forced through this channel in order to reduce the temperature of the PV panels and increase their efficiency [1]. The heated air can then be used for thermal storage or in a heat pump. In this study, natural convection was used inside the air channel in order to reduce the energy requirement of fans to force the air through the BIPV/T system. The advantages of PV/T systems has been reviewed by Kumar and Rosen [2]. They convert solar energy into electricity and heat simultaneously, therefore increasing the overall efficiency over separate solar thermal and PV collectors.

There have been numerous studies on BIPV/T systems [3-8]. Most of these studies have involved conducting experiments to analyze the performance of the BIPV/T system and then develop a simplified mathematical model. Kamel and Fung [9] investigated a PV/T system coupled to a heat pump using a mathematical model. They presented a performance analysis of the air source heat pump based on different duct designs and different PV arrangements. They found that having a longer run for the air channel compared to the PV array width produced more thermal energy with minimal effect on the electrical production. For instance, a 5 high × 3 wide PV panel configuration has a 9.3% higher BIPV/T efficiency than a 3 high × 5 wide configuration.

An experimental study was conducted by Candanedo et al. [10] which developed heat transfer correlations for the top and bottom surface inside a BIPV/T system with forced convection. Correlations were developed for a BIPV/T system at a tilt angle of between 30° and 45° and a Reynolds number between approximately 250 and 7000. They found that existing forced convection correlations predicted lower heat transfer from the PV panel inside the air channel of the BIPV/T.

Liao et al. [11] performed a numerical and experimental study of a BIPV/T system. The realizable k-ε turbulence model was used in a two-dimensional numerical model. The boundary conditions in the numerical model were determined from the measured temperatures of the PV and insulation from the experimental data. Velocity profiles were obtained using particle image velocimetry, which the numerical model was in good agreement with. Convective heat transfer coefficients were developed for the PV and insulation. Due to leading edge effects and the turbulent nature of the flow, the convective heat transfer coefficients were higher than expected.

Getu et al. [12] conducted a CFD study of an air based BIPV/T system using two amorphous PV panels. This paper utilized a similar numerical model to the current study to predict the temperatures of the PV panel, air channel, and insulation. A horizontal orientation was investigated using air velocities between 0.5 and 2.0 m/s. Experimental data from the Solar Simulator Laboratory at Concordia University was used to validate the numerical model. Both k-ε and k-ω turbulence model were tested using a two-dimensional model. It was determined that the k-ε turbulence model yielded the best agreement with the air channel and insulation temperatures and the k-ω turbulence model yielded the best agreement with the PV temperature. At lower air

velocities, due to the low Reynolds number, the numerical results over-predicted the temperatures.

Roeleveld et al. [13] have recently developed a numerical model of a BIPV/T system and validated it against some experimental data obtained by the Solar Simulator Laboratory at Concordia University. Three orientations of horizontal, 45°, and vertical were used with two flowrates of 174 kg/h and 232 kg/h. The temperature profiles inside the air channel were compared between the numerical results and the experimental data. Overall, they showed good agreement. The current paper is an extension of this study that utilizes natural convection inside the channel.

In this study, a CFD model was developed to investigate natural convection inside a BIPV/T system. The BIPV/T system consists of mono-crystalline PV panels with a transparent backing and insulation and plywood as the building structure. Results were obtained at two different orientations of 45° and 90°. The numerically predicted temperature and heat transfer results were compared between these two orientations. Also, the natural convection results were compared with some forced convection cases.

CFD SIMULATION

Based on the experiments carried out in the Solar Simulator Laboratory at Concordia University [14], a numerical model was developed for a BIPV/T system. It consisted of two PV panels mounted above a layer of insulation and plywood separated by an air channel. Figure 1 shows a schematic of the BIPV/T. The dimensions of the BIPV/T were 2.039 m long by 0.529 m wide by approximately 87 mm thick. A schematic of the PV panel is shown in Figure 2. Five layers of various materials make up the PV panels, which included tempered glass, mono-crystalline silicon PV cells, two adhesive layers and the transparent backing material. The air channel thickness, b, was 45 mm and the thickness of the PV panel, t_{PV}, was 4 mm. Typical construction materials of extruded polystyrene insulation and plywood made up the other side of the BIPV/T. The thicknesses were t_{INS} = 25.4 mm (1 in) and t_{ply} = 12.7 mm (0.5 in).

A numerical model was created in the commercial multi-physics finite element analysis software COMSOL Multiphysics [15] using these dimensions. A two-dimensional model with temperature dependent air properties and a k-ω turbulence model was used. The boundary conditions on the outside of the PV panel included a heat flux of the measured solar radiation, surface to ambient radiation and convective heat transfer due to the wind. The solar radiation from the experiments was q_{solar} = 1030 W/m^2. For the surface to ambient radiation, q_{rad}, the glass had an emissivity of 0.89 and the sky temperature, T_{sky}, was approximately 14 °C. The convective heat transfer due to the wind, h_w, was calculated from Duffie and Beckman [16]:

$$h_{wind} = 0.86\, Re_{Lc}^{0.5}\, Pr^{1/3}\, \frac{k_f}{Lc} \qquad (1)$$

where k_f was the thermal conductivity of the outside air, Pr was the Prandtl number of the outside air, and Re_L was the Reynolds number based on the wind speed. It should be noted that Lc refers to the hydraulic diameter of the PV panel (i.e. Lc = 4 × (plate area) / (plate circumference)). The air properties were evaluated at the ambient temperature of the outside air, T_∞, and the wind speed was 2.2 m/s for the experiments. On the backside of the BIPV/T, a natural convective heat transfer coefficient was used (h_{nat} = 2.8 W/(m^2 K)). The PV panel produced electricity, which reduced the total amount of heat transfer through the BIPV/T system. In order to

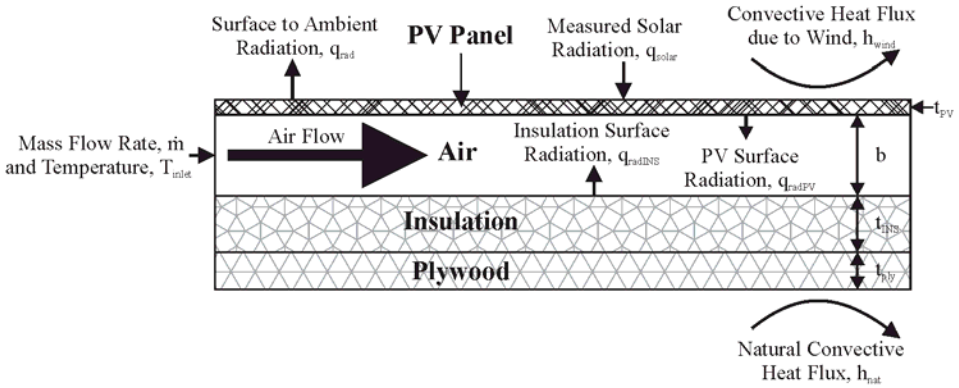

Figure 1: Schematic of the BIPV/T system.

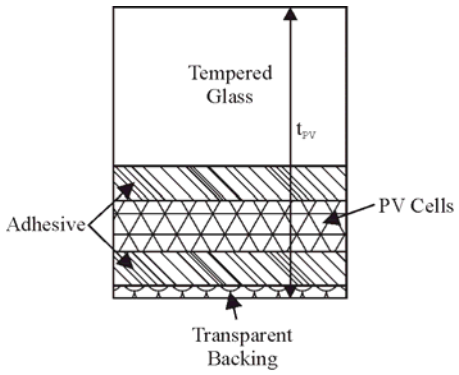

Figure 2: Schematic of the PV panel.

account for this, a volumetric heat absorption was applied to the mono-crystalline silicon PV cells layer. It is known that the efficiency of the PV panels is affected by their temperature. Therefore, the PV panel efficiency, η_{panel}, was calculated by:

$$\eta_{panel} = \eta_{ref}\left[1 - C\left(T_{PV} - T_{ref}\right)\right] \quad (2)$$

where η_{ref} was the reference panel efficiency at the reference temperature, T_{ref} was the reference temperature, T_{PV} was the average temperature of the PV panels and C was the temperature coefficient of the PV panel. The electrical power output by the PV panels, E, was then calculated from:

$$E = \eta_{panel} \cdot q_{solar} \cdot L \cdot W \quad (3)$$

This was input as the volumetric heat absorption.

The air inlet temperature, T_{inlet}, and a pressure inlet were used as inputs for the air inlet in the numerical model. (For validation of the experimental cases, the inlet velocity was specified instead of a pressure inlet.) The turbulence intensity and turbulence length scale were also defined. The turbulence intensity of l_T = 15% was used and the turbulence length scale was calculated to be 0.07 × hydraulic diameter of the air channel. A pressure outlet and outflow were used at the outlet of the air channel. The direct integration surface to surface radiation model was used between the back of the PV panel and the front of the insulation inside the air channel. The emissivity of the back of the PV layer was 0.89 and the emissivity of the insulation was 0.5. A volume force was also added to the air channel in the numerical model to account for buoyancy forces.

The heat transfer coefficients were defined as follows:

$$h_{PV} = \frac{Q_{PV}}{L \cdot W \cdot \left(T_{PV} - T_{inlet}\right)} \quad (4)$$

$$h_{INS} = \frac{Q_{INS}}{L \cdot W \cdot \left(T_{INS} - T_{inlet}\right)} \quad (5)$$

where h_{PV} was the heat transfer coefficient of the backside of the PV layer, Q_{PV} was the heat transfer from the PV layer, h_{INS} was the heat transfer coefficient of the insulation layer, Q_{INS} was the heat transfer from the insulation layer, and T_{INS} was the average insulation temperature. The Nusselt number was defined as:

$$Nu = \frac{\left(Q_{PV} + Q_{INS}\right)b}{2LW\overline{\Delta T}k} \quad (6)$$

where the characteristic temperature difference was:

$$\overline{\Delta T} = \left(T_{PV} + T_{INS}\right)/2 - T_{inlet} \quad (7)$$

and k was the thermal conductivity based on the average temperature in the channel, $T_f = (0.5\,(T_{PV} + T_{INS}) + T_{inlet})\,/\,2$.

To ensure that the numerical solution was grid independent, a grid sensitivity study was performed. Three grid sizes of 68,500, 33,335 and 15,225 elements were used with a $\dot{m}$ = 232 kg/h and the vertical orientation. A Richardson extrapolation [16] was performed using the heat transfer coefficient of the PV (h_{PV}) as the critical variable. The numerical uncertainty was 1.5% for the grid size of 68,500 elements. Table 1 shows the grid sensitivity study, where the difference between the coarse and fine grid was 1.6%. Therefore, the grid size of 68,500 elements was determined to be sufficient for this study.

EXPERIMENT

The Solar Simulator Laboratory at Concordia University carried out some experiments of forced convection

Table 1: Grid sensitivity study for $\dot{m}$ = 232 kg/h at a vertical orientation.

Grid Size	Number of Elements	Heat Transfer Coefficient of PV h_{PV} (W/m^2)
Fine	68,500	15.55
Medium	33,335	15.46
Coarse	12,225	15.31

inside a BIPV/T system. The experimental model was constructed to the specifications previously discussed in the CFD simulation section. These experiments used two different mass flow rates of approximately 174 kg/h and 232 kg/h inside the air channel and two different orientations of 45° and vertical (90°). The temperature profiles of the backside of the PV panels, the surface of the insulation, and the centerline of the air channel were measured using thermocouples. The numerical model was validated using this experimental data.

Figures 3 and 4 show a comparison of the temperature profiles between the experimental data and the numerical results for two different cases. Figure 3 shows a 45° orientation at 174 kg/h and Figure 4 shows a vertical orientation at 232 kg/h. Three temperature profiles are shown in each figure are: a) the backside of the PV panel, b) the insulation surface, and c) the centerline of the air channel. Overall the numerical predictions showed good agreement with the experiment data. It should be noted that in the experimental data the temperature drops at the center of the PV panel. This was due to the packing factor of the PV cells between the two PV panels. There was a gap in the PV cells at the joint between the two PV panels that allowed the solar radiation to transmit through the PV layer because of the transparent backing. Further validation of the forced convection cases were presented in Roeleveld [13].

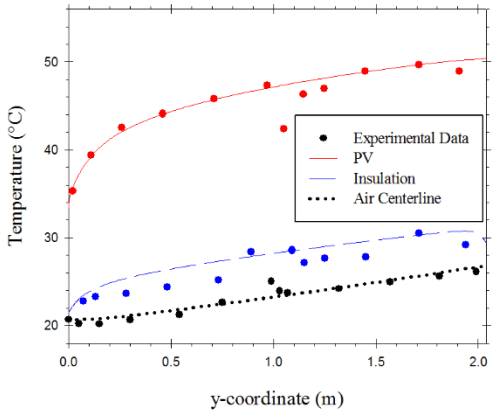

Figure 3: Comparison of the temperature profiles between the numerical results and experimental data for a 45° orientation and mass flow rate of 174 kg/h.

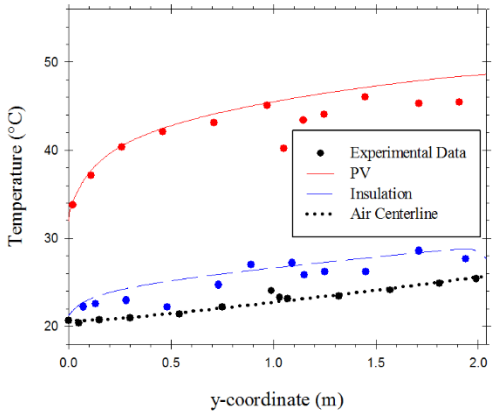

Figure 4: Comparison of the temperature profiles between the numerical results and the experimental data for a vertical orientation and mass flow rate of 232 kg/h.

RESULTS

Figure 5 shows the temperature profiles for natural convection inside the air channel at both an orientation of 45° and 90°. As expected, the temperature profiles were higher in the natural convection cases compared to the forced convection cases.

The natural convection cases were compared to the overall channel average Nusselt number correlation by Raithby and Hollands [18]:

$$Nu = \left[\left(\frac{4R_T^2 + 7R_T + 4}{90(1+R_T)^2} Ra \right)^{-1.9} + \left(0..680 Ra^{\frac{1}{4}} \right)^{-1.9} \right]^{\frac{1}{-1.9}} \quad (8)$$

where the temperature ratio was defined as:

$$R_T = \frac{T_{INS} - T_\infty}{T_{PV} - T_\infty} \quad (9)$$

The Rayleigh number was:

$$Ra = \frac{g\beta\overline{\Delta T}b^4}{\nu\alpha L} \quad (10)$$

where g was the gravitational constant, β was the thermal expansion coefficient, ν was the dynamic viscosity, and α was the thermal diffusivity.

For the vertical orientation, the temperature ratio was R_T = 0.39 and Rayleigh number was Ra = 3622. The overall channel average Nusselt number was calculated to be within 2.8% of the Raithby and Hollands correlation. For the 45° orientation, R_T = 0.42 and Ra = 2661. The Nusselt number was within 5.9% of the Raithby and Hollands correlation.

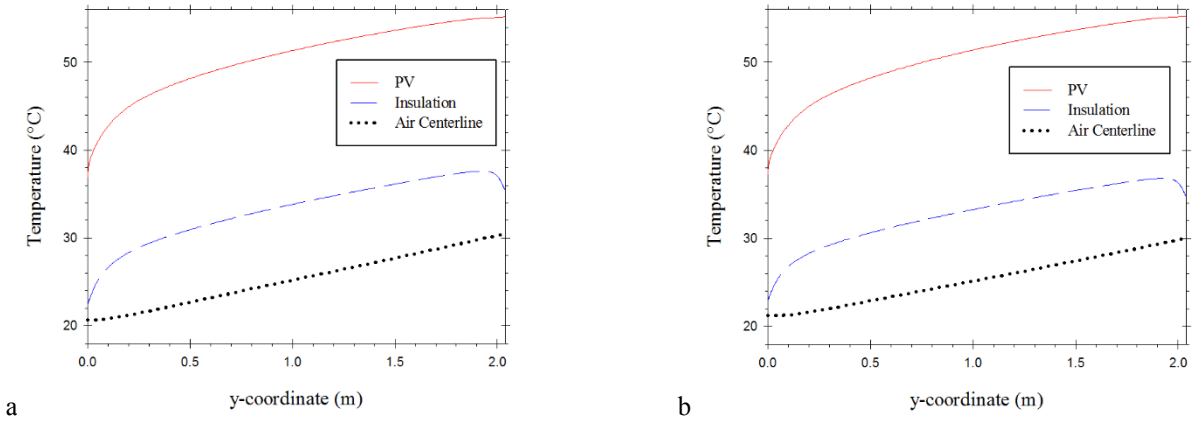

Figure 5: Comparison of the temperature profiles for natural convection at a) a 45° orientation and b) a vertical orientation.

Table 2 shows a comparison of the numerically predicted temperatures for both the forced and natural convection cases. In vertical case, the flowrate was approximately 12 kg/h higher than the 45° case. This corresponded to a higher average air velocity of 0.96 m/s for the vertical case compared to 0.83 m/s for the 45° case. For both natural convection cases, the PV temperature was the same, but the average insulation temperature was ~0.45 °C higher for the 45° case. Also, the air temperature at the outlet was ~0.35 °C warmer in the 45° case.

A comparison of the heat transfer coefficients, the heat transfer from the air channel and the overall BIPV/T efficiency is shown in Table 3. It should be noted that both the PV and insulation surfaces were heating the air in the channel due to the radiation exchange between the PV and insulation. Comparing the two natural convection cases, the vertical orientation had better performance than the 45° orientation. The heat transfer coefficients of both the PV and insulation were higher in the vertical case. Also, there was more heat transfer from the air channel in the vertical case. The overall channel BIPV/T efficiency is defined as:

$$\eta_{BIPV/T} = \frac{Q_{AIR} + E}{q_{solar} \cdot L \cdot W} \quad (11)$$

The 45° case had a 37.0% overall BIPV/T efficiency compared to the vertical case which had an overall BIPV/T efficiency of 39.3%.

Comparing the natural convection cases to the forced convection cases, the mass flowrate was approximately half of the forced convection case of 174 kg/h. In the natural convection cases, the PV temperature was

Table 2: Comparison of the numerically predicted temperatures for all cases.

Orientation	Type of Convection	Mass Flow Rate	Average Air Velocity	Reynolds Number	Average PV Temperature	Average Insulation Temperature	Average Air Temperature at Outlet
		$\dot{m}$ kg/h	u m/s	Re	T_{PV} °C	T_{INS} °C	T_{outlet} °C
45°	Natural	84	0.83	4476	50.6	33.28	33.29
45°	Forced	174	1.7	9295	46.3	27.94	29.22
45°	Forced	247	2.4	13186	43.8	25.69	27.31
Vertical	Natural	98	0.96	5218	50.6	32.82	32.94
Vertical	Forced	174	1.7	9264	47.1	28.66	29.85
Vertical	Forced	232	2.3	12365	44.7	26.42	27.95

Table 3: Comparison of the numerically predicted heat transfer coefficients for all cases.

Orientation	Type of Convection	Mass Flow Rate	Reynolds Number	Heat Transfer Coefficient of PV	Heat Transfer Coefficient of Insulation	Heat Transfer of Air Channel	Overall BIPV/T Efficiency
		$\dot{m}$	Re	h_{PV}	h_{INS}	Q_{AIR}	$\eta_{BIPV/T}$
		kg/h		W/(m^2 K)	W/(m^2 K)	W	%
45°	Natural	84	4476	7.89	2.31	295.4	37.0
45°	Forced	174	9295	12.85	4.45	415.4	48.0
45°	Forced	247	13186	16.26	5.88	481.1	54.0
Vertical	Natural	98	5218	8.68	2.73	320.3	39.3
Vertical	Forced	174	9264	12.81	4.52	418.3	48.3
Vertical	Forced	232	12365	15.55	5.67	472.0	53.2

approximately 3 – 4 °C warmer than the 174 kg/h cases, which in turn was ~2.5 °C warmer than the 232 kg/h cases. This showed that there will be less electricity production from the PV panels in the natural convection cases compared to the forced convection cases. The air temperature at the outlet of the air channel was also approximately 3 – 4 °C warmer for the natural convection cases compared to the 174 kg/h cases. The 174kg/h cases had an outlet air temperature ~2 °C higher than the 232 kg/h cases.

The heat transfer coefficients of the PV and insulation for the natural convection cases were approximately half of the forced convection cases of 232 kg/h. There was also approximately 110 W more heat transfer from the air channel between the natural convection cases and the 174 kg/h cases, which was approximately 50 W less than the 232 kg/h cases. The overall BIPV/T efficiency was approximately 54% for the 232 kg/h case, compared to approximately 48% for the 174 kg/h case, which was approximately 10% higher than the overall BIPV/T efficiency of the natural convection cases.

CONCLUSIONS

A numerical model was developed to determine the heat transfer inside a BIPV/T that utilizes natural convection inside the air channel. The model consisted of a two PV panels, an air channel, and typical building construction of insulation and plywood. A k-ω turbulence model was used to study the natural convection inside the air channel. Typical boundary conditions of a BIPV/T system were used, such as a solar heat flux, radiation exchange with the ambient, and convective heat transfer due to the wind on the PV panels. On the backside of the BIPV/T, natural convection was used. Forced convection results were obtained from the Solar Simulator Laboratory at Concordia University, which were used to validate the CFD model. The numerically predicted temperature profiles showed good agreement with the experimental data. Natural convection inside the air channel was studied at two orientations of 45° and 90°. The vertical case had a higher flowrate and overall BIPV/T efficiency compared to the 45° case. It was shown that the mass flow rates of the natural convection cases were approximately half of the 174 kg/h cases and that the PV panel temperature increases by ~3 – 4 °C. The heat transfer coefficients of the natural convection cases are also approximately half of the 232 kg/h cases.

ACKNOWLEDGEMENTS

This research was supported by Connect Canada through the Ontario Centres of Excellence (OCE), NSERC Engage through the Natural Sciences and Engineering Research Council of Canada (NSERC), s2e Technologies Inc., and Strathcona Energy Group.

NOMENCLATURE

b	air channel thickness
C	temperature coefficient of the PV panels
E	electrical output
g	gravitational constant
h_{INS}	heat transfer coefficient of the insulation
h_{nat}	interior natural convective heat transfer coefficient
h_{PV}	heat transfer coefficient of the PV
h_{wind}	heat transfer coefficient due to the wind
k	thermal conductivity at T_f
k_f	thermal conductivity at ambient
L	length of the BIPV/T
Lc	hydraulic diameter of the PV panels
l_T	turbulence intensity

$\dot{m}$	mass flowrate of air
Nu	overall channel average Nusselt number
Pr	Prandtl number of the outside air
Q_{AIR}	heat transfer from the air channel
Q_{INS}	heat transfer from insulation
Q_{PV}	heat transfer from PV
q_{rad}	surface to ambient radiation
q_{radINS}	heat transfer due to radiation from the insulation
q_{radPV}	heat transfer due to the radiation from the PV
q_{solar}	solar radiation
Ra	Rayleigh number inside the air channel
Re	Reynolds number inside the air channel
Re_L	Reynolds number based on wind speed
$\underline{R_T}$	temperature ratio
ΔT	characteristic temperature difference
T_∞	ambient temperature
T_f	average temperature of the air channel
T_{inlet}	inlet air temperature
T_{INS}	average temperature of the insulation
t_{INS}	insulation thickness
T_{oulet}	air temperature at the exit of the BIPV/T
t_{ply}	plywood thickness
T_{PV}	average temperature of the PV panels
t_{PV}	thickness of the PV panel
T_{ref}	reference temperature
T_{sky}	sky temperature
W	width of the BIPV/T
α	thermal diffusivity
β	thermal expansion coefficient
$\eta_{BIPV/T}$	overall BIPV/T efficiency
η_{panel}	PV panel efficiency
η_{ref}	reference panel efficiency at the reference temperature
ν	dynamic viscosity

REFERENCES

[1] Zondag H.A. (2008), 'Flat-Plate PV-Thermal Collectors and Systems: A Review', *Renewable and Sustainable Energy Reviews,* 12 891-959.

[2] Kumar R. and Rosen M.A. (2011) 'A Critical Review of Photovoltaic-Thermal Solar Collectors for Air Heating', *Applied Energy*, 88 3602-3614.

[3] Nagano K., Mochida T., Shimakura K., Murashita K. and Takeda S. (2003) 'Development of Thermal-Photovoltaic Hybrid Exterior Wallboards Incorporating PV Cells in and Their Winter Performance', *Solar Energy Materials & Solar Cells,* 77 265-82.

[4] Anderson T.N., Duke M., Morrison G.L. and Carson J.K. (2009) 'Performance of a Building Integrated Photovoltaic/Thermal (BIPVT) Solar Collector', *Solar Energy*, 83 445-55.

[5] Agrawal B. and Tiwari G.N. (2010) 'Optimizing the Energy and Exergy of Building Integrated Photovoltaic Thermal (BIPVT) Systems under Cold Climatic Conditions', *Applied Energy,* 87 417-26.

[6] Pantic S., Candanedo L. and Athienitis A.K. (2010) 'Modeling of Energy Performance of a House with Three Configurations of Building-Integrate Photovoltaic/Thermal Systems', *Energy and Buildings,* 42 1779-89.

[7] Chen Y., Athienitis A.K. and Galal K. (2010) 'Modeling Design and Thermal Performance of a BIPV/T System Thermally Coupled with a Ventilated Concrete Slab in a Low Energy Solar House: Part 1, BIPV/T System and House Energy Concept', *Solar Energy*, 84 1892-907.

[8] Kamel R.S. and Fung A.S. (2014) 'Theoretical Estimation of the Performance of a Photovoltaic-Thermal Collector (PV/T) System Coupled with a Heat Pump in a Sustainable House in Toronto', *ASHRAE Transactions,* 120179-191.

[9] Candanedo L., Athienitis A.K. and Park K.W. (2000) 'Convective Heat Transfer Coefficients in a Building-Integrated Photovoltaic/Thermal System', *Journal of Solar Engineering*, 133 021002-1-14.

[10] Liao L., Athienitis A.K., Candanedo L., Park K.W., Poissant Y. and Collins M. (2007) 'Numerical and Experimental Study of Heat Transfer in a BIPV-Thermal System', *Journal of Solar Engineering*, 129 423-30.

[11] Naewngerndee R., Hattha E., Chumpolrat K., Sangkapes T., Phonsitong J. and Jaikla S. (2011) 'Finite Element Method for Computational Fluid Dynamics to Design Photovoltaic Thermal (PV/T) System Configuration', *Solar Energy & Solar Cells*, 95 390-3.

[12] Getu H., Yang T., Athienitis A.K. and Fung A. (2014) 'Computational Fluid Dynamics (CFD) Analysis of Air Based Building Integrated Photovoltaic Thermal (BIPV/T) Systems for Efficient Performance', In *eSIM 2014 Conference Proceedings*, Ottawa, Canada. 18 pages.

[13] Roeleveld D., Hailu G., Fung A.S., Naylor D., Yang T., and Athienitis A.K. (2015) 'Validation of

Computational Fluid Dynamics (CFD) Model of a Building Integrated Photovoltaic/Thermal (BIPV/T) System', *Energy Procedia*, 78 1901-1906.

[14] Yang T. and Athienitis A.K. (2014) 'A Study of Design Options for a Building Integrated Photovoltaic/Thermal (BIPV/T) System with Glazed Air Collector and Multiple Inlets', *Solar Energy,* 104 82-92.

[15] COMSOL Multiphysics 4.3b (Version 4.3.2.152) (2013) [software].

[16] Duffie J.A. and Beckman W.A. (2013) *Solar Engineering of Thermal Processes, 4th ed.,* John Wiley & Sons, Inc.

[17] Celik I.B., Ghia U., Roache P.J., Freitas C.J., Coleman H. and Raad P.E. (2008) 'Procedure for Estimation and Reporting of Uncertainty Due to Discretization in CFD Applications', *Journal of Fluids Engineering*, 130 1-4.

[18] Raithby G.D. and Hollands K.G.T. (1998) 'Natural Convection', in: *Handbook of Heat Transfer*, ed. Rohsenow W.M. Harnett J.P. and Cho Y.I., Mcgraw-Hill, 4.32-4.45.